JOURNAL OF PROPULSION AND POWER
Vol. 23, No. 1, January–February 2007

Turbulence Measurements and Analysis in a Multistage Axial Turbine

Luca Porreca,* Marc Hollenstein,† Anestis I. Kalfas,‡ and Reza S. Abhari§
Swiss Federal Institute of Technology, 8092 Zürich, Switzerland

DOI: 10.2514/1.20022

This paper presents turbulence measurements and detailed flow analysis in an axial turbine stage. Fast response aerodynamic probes were used to resolve aperiodic fluctuations along the three directions. Assuming incompressible flow, the effective turbulence level and Reynolds stress are retrieved by evaluating the stochastic velocity component out of the measured time-resolved pressure and flow angle fluctuations along the streamwise, radial, and circumferential direction. A comparison between turbulence intensity and measured total pressure shows that flow structures with higher turbulence level are identified in the region of loss cores at the exit of the second stator passage. Turbulence intensity is evaluated under isotropic and nonisotropic assumption in order to quantify the departure from isotropic conditions. The measurements show that locally the streamwise fluctuating component can be twice bigger than the radial and tangential component. The current analysis shows that multisensor fast response aerodynamic probes can be used to provide information about the mean turbulence levels in the flow and the Reynolds stress tensor, in addition to the measurements of unsteady total pressure loss.

Nomenclature

c	=	absolute velocity vector
e	=	mean unit vector in the secondary flow definition
p	=	static pressure
p_d	=	dynamic head
s, θ, r	=	streamwise, circumferential, and radial directions
T/T_0	=	blade passing period fraction
t	=	time
u	=	streamwise velocity component
$\tilde{u}$, $\tilde{v}$, $\tilde{w}$	=	periodic velocity component: phase-lock averaged
u', v', w'	=	stochastic (aperiodic) velocity components
v	=	circumferential velocity component
w	=	radial velocity component
α	=	yaw angle
β	=	pitch angle
Δx	=	absolute uncertainty of quantity x
ρ	=	density

Subscripts/superscripts

1	=	probe position 1
iso	=	isotropic assumption
NS	=	nonsimultaneous
sec	=	secondary flow vector

Presented at the International Symposium on Airbrteathing Engines ISABE 2005, Munich, Germany, 4–9 September 2005; received 13 September 2005; revision received 3 February 2006; accepted for publication 14 February 2006.

*Research Assistant, Turbomachinery Laboratory; porreca@lsm.iet.mavt.ethz.ch (corresponding author).
†Research Assistant, Institute of Mechanical Systems.
‡Senior Scientist, Turbomachinery Laboratory; current address Aristotle University of Thessaloniki, Greece. Member AIAA.
§Professor, Head of the Department, Turbomachinery Laboratory.

I. Introduction

TURBULENCE modeling is still a critical issue in fluid dynamics. Despite the recent progress of design tools in modern fluid machinery, the use of appropriate turbulence modeling is instrumental in further development and improvement of internal flows machinery applications. To validate numerical tools and turbulence models, a large number of experimental investigations have been performed in wind tunnels with simple geometry and under flow conditions involving few disturbances. In those cases, velocity measurements rather than pressure are performed using hot wire anemometry or, more recently, optical methods such as laser Doppler velocimetry (LDV) or particle image velocimetry (PIV). With these techniques, unsteadiness on the three spatial directions can be resolved up to a relatively large frequency.

Flow in a turbomachinery environment is, however, highly unsteady and three dimensional as a result of periodic chopping of the wake, secondary flow vortices interaction, and combustion dynamics. Therefore, particularly in low aspect ratio blading, common isotropic turbulence models validated in simple geometry may not be suitable. Several investigations were performed on turbine blading focusing on the effect of turbulence intensity on the heat transfer [1,2], secondary flows development and transition [3–6]. Ristic et al. [7] and Xiao and Lakshminarayana [8] performed detailed measurements using LDA inside a turbine rotor where a high level of anisotropy has been reported in the wake and secondary flow region. They also measure high differences in the shear stress components concluding that the isotropic eddy viscosity model used in numerical computations could be invalid in these regions. Matsunama and Tsutsui [9] performed also measurements with LDV inside a turbine rotor focusing on the stator/rotor interaction. Generally, however, very little has been published in order to quantify the departure from the isotropic conditions in a multistage turbine environment.

While all those studies are based primarily on hot wire anemometry measurements, the present work is based on the extraction of turbulence parameters out of unsteady pressure probes. Previous works have been focused on using fast pressure probes to measure turbulence; Heneka [10] developed a 4 sensor probe able of measure turbulent quantities, Ruck [11] using similar instrumentations performed measurements in a low pressure turbine. Wallace and Davies [12] performed turbulent measurements with a calibrated single pitot mounted pressure transducer in a rotating frame. Gossweiler et al. [13] measured with a 4-sensor fast response pressure probe in a fully developed turbulent pipe flow. Results were

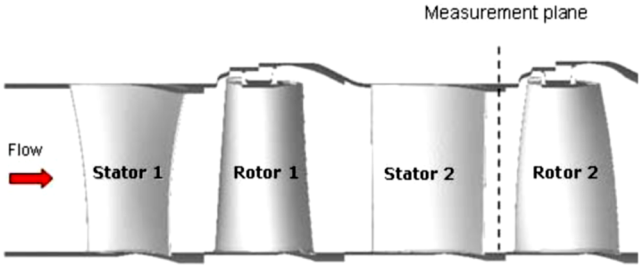

Fig. 1 Meridional view of the 2 stages axial turbine LISA.

compared with hot wire data from Laufer [14] showing general agreement with maximum deviations up to 18%.

Koeppel [15] measured time-resolved flow quantities in a centrifugal compressor using fast response aerodynamic probe (FRAP) and LDA technology. Turbulence intensity was derived from the unsteady pressure signal assuming isotropic conditions and incompressible flow. Comparison of the turbulence level evaluated with both measurement technology showed a very good qualitative agreement and resulted in an offset of the FRAP measurement of about 4% in whole measurement area with respect to the LDA measurements.

This paper follows a series of studies on unsteady flows in a multistage environment, conducted on the same shrouded turbine geometry and focused on blade interaction [16–19]. A methodology is proposed to derive turbulence quantities along the three spatial directions. An analysis of the unsteady phenomena is presented focused on flow structures behind the second stator row. The degree of anisotropy in a multistage turbine stage is also quantified. Measurements are performed using a 2-sensors miniaturized cylindrical fast response aerodynamic probe developed at the Turbomachinery Laboratory at the Swiss Federal Institute of Technology in Zurich (ETHZ) [20].

II. Experimental Method

A. Research Facility

The experimental investigation was performed on the research turbine "LISA" at the Turbomachinery Laboratory of the ETHZ. The facility can accommodate a maximum of two stages of an axial turbine. The air-loop is of a closed type and includes a radial compressor, a two-stage water to air heat exchanger and a calibrated venturi nozzle for accurate mass flow measurements. A dc generator absorbs the turbine power and controls the rotational speed of the turbine shaft. The first and the second rotor are mechanically decoupled by a twin spool shaft design. A set of independent torque meters allows to derive separately the torque of both stages. To achieve the same rotational speed, both shafts are coupled again before the dc generator. A sketch of the turbine test section is presented in Fig. 1.

The turbine design allows quick and precise assembly and an easy access to the measurement planes. A number of different intrusive (probes) and nonintrusive measurement PIV techniques are applied. The facility is equipped with a 4-axis numerically controlled positioning system with ultrahigh precision in every direction. The turbine is normally operated at constant pressure difference across the stages. The turbine entry temperature is controlled to an accuracy of 0.3% and the revolutions per minute are kept constant by the dc generator with a range of $\pm 0.02\%$ (± 0.5 rpm). The main operational parameters of the facility are listed in Table 1. The test case under investigation is representative of a partially shrouded axial turbine for power generation. The partial shroud has two vertical fins and a shroud platform with cutbacks at leading and trailing edges. The tip clearance in both rotors is 1% of the blade span.

Table 1 Main parameter of LISA 2-stages axial turbine research facility

Rotor speed (rpm)	2625
Overall pressure ratio	1.38
Mass flow (kg/s)	10.65
Blade count (stator/rotor)	42/42
Aspect ratio	1.8
Outer tip diameter (m)	0.8
Mach number (stator/rotor)	0.35/0.1
Reynolds number (rotor)	2×10^5

B. Measurement Technology

Flow parameters including total and static pressure, flow angles velocity components and Mach numbers are measured at frequencies up to 40 kHz using 2-sensor fast response aerodynamic probe (2S-FRAP). This probe is a modified version of the conventional single sensor probe already used in previous investigations [16–18] and has a second sensor sensitive of pitch angle variation of the flow. The dimensions of each piezoresistive sensor are 0.4×0.8 mm, the distance between the two sensors is approximately 2.2 mm and the tip diameter of the probe is 1.8 mm. This concludes that the sensing area of the probe is of the order of 3.9 mm^2.

FRAP probe technology provides also unsteady temperature measurements at very low frequency (up to 10 Hz). The absolute uncertainties of the used probe techniques are listed in Table 2. Temperature measurements obtained with FRAP are affected by an absolute uncertainty of the order of ± 0.3 K.

This paper is focused on the measurements performed downstream the exit of the second stator blades row. the measurement grid comprises 1240 points distributed uniformly in the circumferential direction every 3.5% pitch (31 point in 1.1 pitches) and 40 points in the radial direction, clustered toward the end walls. Owing to an improved and faster probe traversing system, the data acquisition of one measurement plane currently lasts about 7 h while the turbine pressure drop is stable within 0.3%. Data from the probe sensors are sampled at 200 kHz corresponding to 109 samples each blade passing period. Phase locking averaging data procedure is done over 80 rotor revolutions.

III. Data Reduction

A. Turbulence

The time dependent variables in a turbulent flow are commonly split into periodic and a stochastic (aperiodic) signal using the Reynolds decomposition [Eq. (1)]. In the probe relative frame of reference shown in Fig. 2, the absolute flow velocity can be written as

$$c(t) = \tilde{c} + c'(t) \tag{1}$$

where $\tilde{c}$ is the periodic velocity. This component is a function of the rotor blade position and is calculated using the phase locking averaging procedure; $c'(t)$ is the stochastic unresolved unsteadiness due to turbulence (aperiodic).

The turbulent stresses are used to form the Reynolds stress tensor in terms of velocity fluctuations on the three spatial directions. The conventional definition of the turbulence intensity level (Tu) is [Eq. (2)]:

$$\mathrm{Tu} = \sqrt{\frac{\overline{u'^2} + \overline{v'^2} + \overline{w'^2}}{3\tilde{c}^2}} \tag{2}$$

B. Turbulence Measurements with Fast Response Aerodynamic Probes

The measurement probe used has two piezoelectric sensors located on the stem and on the inclined surface at the tip of the probe,

Table 2 Uncertainty bandwidth of the 2S-FRAP

	ϕ	β	Pt	P_S	Ma
2S-FRAP	0.3 deg	0.3 deg	100 Pa	150 Pa	0.4%

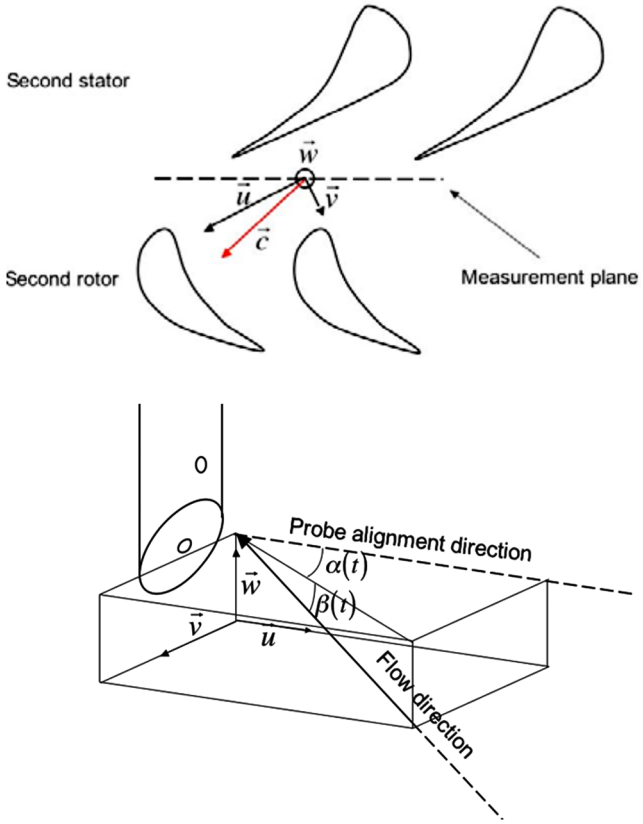

Fig. 2 Probe relative coordinate system and definitions.

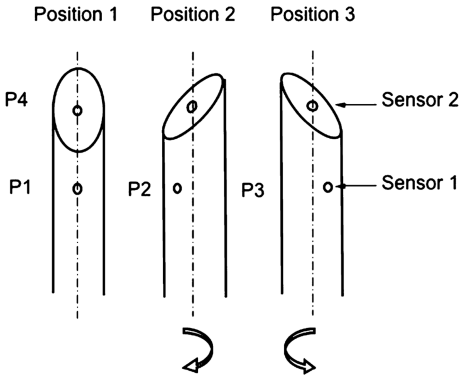

Fig. 3 Measurement procedure of the 2S-FRAP.

respectively, as shown in Fig. 3. In each measurement point, the probe is turned in three positions. In position 1 the sensors are aligned with the mean direction of the flow evaluated using data form previous measurements [5 hole probe (5 HP) measurements]. In position 1, unsteady signal from both sensors is acquired simultaneously (P1 and P4). Positions 2 and 3 are necessary in order to measure flow yaw angle by acquiring data only from sensor 1 (P2 and P3).

All four pressure signals are brought together in a set of calibration coefficients representing a dimensionless yaw, pitch, total, and static pressure. The periodic part of the signal is derived using the phase-lock averaging procedure over 80 events. The stochastic unresolved part of the signal is retrieved from the difference between the actual measured value and the periodic value.

The flow is considered as incompressible (Mach number between 0.1 and 0.3) and the angle variations in each measurement point are limited to ± 5 deg over one blade passing period. Because the probe is positioned in the direction of the flow, in the stagnation point (measurement position 1) the total pressure can be written as [Eq. (3)]:

$$p_1(t) = p_s(t) + \tfrac{1}{2}\rho u(t)^2 \tag{3}$$

therefore:

$$u(t) = \sqrt{\frac{2[p_1(t) - p_s(t)]}{\rho}} = \sqrt{\frac{2p_d(t)}{\rho}}$$

If the velocity is decomposed into periodic and stochastic part then

$$u'(t) = u(t) - \tilde{u} = \sqrt{\frac{2p_d(t)}{\rho}} - \sqrt{\frac{2\tilde{p}_d}{\rho}} \tag{4}$$

$$u'^2 = \frac{2}{\rho}(p_d + \tilde{p}_d - 2\sqrt{p_d \tilde{p}_d}) \tag{5}$$

Averaging the measured points in the pitch, data show that static pressure fluctuations can be considered small with respect to the dynamic head ($p_s'/\tilde{p}_d < 8\%$). The dynamic head can be separated into steady and fluctuating part. Expanding the term $\sqrt{p_d}$ into a Taylor series, the previous expression can be written as [Eq. (6)] (Ruck [11])

$$\overline{u'^2} = \frac{1}{2\rho}\frac{\overline{p_1'^2}}{\tilde{p}_d} \tag{6}$$

As mentioned before, the probe sensors are aligned with the flow direction. Figure 4 shows the pitchwise averaged periodic velocity $\tilde{v}$ and $\tilde{w}$ with respect to the absolute velocity $\tilde{c}$.

Therefore it can be written that

$$\tilde{v} \ll \tilde{c}, \qquad \tilde{w} \ll \tilde{c}$$

then

$$\tilde{u} \cong \tilde{c}$$

therefore

$$\frac{\overline{u'^2}}{\tilde{c}^2} = \frac{1}{4}\frac{\overline{p_1'^2}}{\tilde{p}_d^2} \tag{7}$$

In the probe relative reference system, the yaw angle can be written as

$$\tan[\alpha(t)] = \tan[\tilde{\alpha} + \alpha'(t)] = \frac{v(t)}{u(t)} = \frac{\tilde{v} + v'(t)}{\tilde{u} + u'(t)}$$

it follows that

$$\tilde{v} \cong 0, \tilde{w} \cong 0 \quad \text{and} \quad \tilde{\alpha} \cong 0, \tilde{\beta} \cong 0$$

therefore the above equation can be simplified as

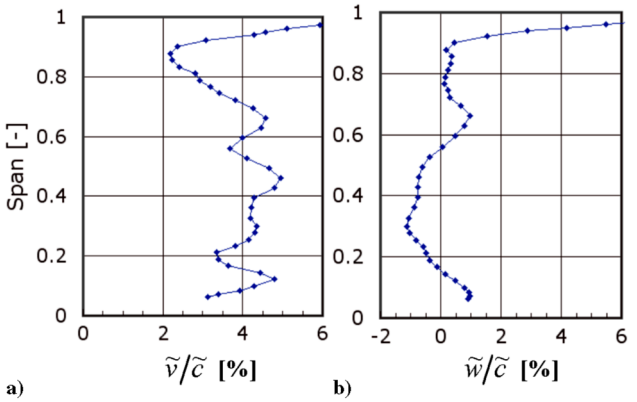

Fig. 4 Ratio between periodic velocity *v* a) and *w* b) with respect to the absolute periodic velocity *c*.

$$\tan[\alpha(t)] = \tan[\alpha'(t)] \cong \alpha'(t) = \frac{v'(t)}{\tilde{c}} \tag{8}$$

An equivalent derivation can be done over the pitch angle, thus the circumferential and radial normal stress components are [Eq. (9)]

$$\frac{\overline{v'^2}}{\tilde{c}^2} = \overline{\alpha'^2} \quad \text{and} \quad \frac{\overline{w'^2}}{\tilde{c}^2} = \overline{\beta'^2} \tag{9}$$

The shear stress component of the Reynolds tensor can be expressed as the product of two velocities fluctuation, respectively. Following the method developed above yields [Eq. (10)]:

$$\frac{\overline{u'v'}}{\tilde{c}^2} = \frac{\overline{\alpha' p'_1}}{2p_d} \qquad \frac{\overline{u'w'}}{\tilde{c}^2} = \frac{\overline{\beta' p'_1}}{2p_d} \qquad \frac{\overline{w'v'}}{\tilde{c}^2} = \overline{\alpha'\beta'} \tag{10}$$

Attention needs to be paid to the evaluation of the term $\overline{v'^2}$ in Eq. (9). As mentioned before, the 2S-FRAP probe is turned in position 2 and 3 to measure flow yaw angle thus yaw angle measurements are evaluated using 3 nonsimultaneous measurements. This procedure is appropriate when evaluating the periodic phase-lock averaged angle $\tilde{\alpha}$, but not valid to calculate the term $\overline{v'^2}$. For this reason $\overline{v'^2}$ is evaluated from the measurements of the terms $\overline{u'^2}$ and $\overline{w'^2}$. From the continuity equations for incompressible flow in cylindrical coordinates, it follows that [Eq. (11)]:

$$\frac{\partial u'}{\partial s} + \frac{1}{r}\frac{\partial v'}{\partial \theta} + \frac{1}{r}\frac{\partial r w'}{\partial r} = 0 \tag{11}$$

Assuming that

$$\frac{\partial}{\partial s} \ll \frac{\partial}{\partial \theta}$$

then

$$v' = -\int \frac{\partial r w'}{\partial r} d\theta + \text{const}(r, \theta) \tag{12}$$

The integration constant is a function of the measurement point position and needs some considerations. As mentioned previously, the evaluation of the yaw angle term $\tilde{\alpha}$ is derived by 3 phase locked nonsimultaneous measurements. Is still possible to define the quantity α'_{NS} resulting from nonsimultaneous measurements as

$$\alpha'_{\text{NS}}(t) = \alpha(t) - \tilde{\alpha} \tag{13}$$

it follows that [see Eq. (9)]

$$\frac{v'_{\text{NS}}(t)}{\tilde{c}} = \alpha'(t) \tag{14}$$

it can be assumed that the flow is phase locked with the blade position and therefore, at the same rotor blade position corresponds, on an average basis, the same turbulent structure. Having in mind this, the constant in Eq. (12) can be defined locally as the value assumed by the quantity v'_{NS} calculated using Eq. (14). Thus

$$v' = -\int \frac{\partial r w'}{\partial r} \, \mathrm{d}\theta + v'_{\text{NS}}(r, \theta) \tag{15}$$

the circumferential term $\overline{v'^2}$ can be computed in all the measurement plane.

C. Uncertainty Analysis

An analysis is carried out in order to quantify the uncertainty of the methodology to evaluate the turbulence quantities. Based on Table 2, the absolute uncertainty of the dynamic head $\tilde{p}_d$ is the square root of the sum of the squared absolute uncertainties of total and static pressure.

$$\Delta\tilde{p}_d = \sqrt{\Delta p^2 + \Delta p_d^2} \cong 180 \text{ Pa}$$

Considering the term in streamwise direction $\overline{u'^2}$ [Eq. (6)], the relative uncertainty of the numerator and denominator is equal to the square root of the sum of the squared relative uncertainties. Therefore:

$$\frac{\Delta\tilde{p}_d^2}{\tilde{p}_d^2} = \sqrt{2}\frac{\Delta\tilde{p}_d}{\tilde{p}_d} \cong 0.032$$

$$\frac{\Delta p'^2}{p'^2} = \sqrt{2}\frac{\Delta p'}{p'} \cong 0.0013$$

Combining both expressions the averaged relative uncertainty on the whole measurement area is equal to

$$\Delta\left(\frac{\overline{u'^2}}{\tilde{c}^2}\right) \Big/ \frac{\overline{u'^2}}{\tilde{c}^2} = 3.3\%$$

Higher uncertainty values up to 5.2% are occurring in the wake and in the secondary flows region due to the lower value of the dynamic head.

Uncertainty in the radial component $\overline{w'^2}$ [Eq. (9)] is affected by the uncertainty on the pitch angle measurements. From the aerodynamic calibration procedure, the absolute error is in the range of ± 0.3 deg for yaw angle calibration range of ± 10 deg. This corresponds with a relative uncertainty of the order of $\pm 2.2\%$. Therefore

$$\frac{\Delta\beta^2}{\beta^2} = \sqrt{2}\frac{\Delta\beta}{\beta} \cong 3.1\%$$

The circumferential normal stress term $\overline{v'^2}$ calculated with the assumption made in the previous section is affected by a higher uncertainty. The assumption made to derive the integration constant in Eq. (9) can results in a high uncertainty on the absolute level. However the level of the fluctuation given by the term $-\int(\partial r w'/\partial r)\, \mathrm{d}\theta$ in Eq. (12) has the same uncertainty of the terms $\overline{w'^2}$.

IV. Results and Discussion

This study focuses on the flow field measured downstream the second stator row. Results are presented as area plots and pitchwise mass averaged profile. Figure 5 shows the time-averaged total pressure coefficient and yaw angle profile on the blade span. At the hub, the passage vortex is established with typical overturning–underturning behavior. This is also responsible for the total pressure reduction at around 10% span. Further up in the radial direction, a marked underturning–overturning behavior is observed at 70% of the span. This feature is caused by the tip passage vortex. The area plot (Fig. 6) shows the time-averaged measured total pressure coefficient together with the time-averaged secondary flow vectors defined as [Eq. (16)]:

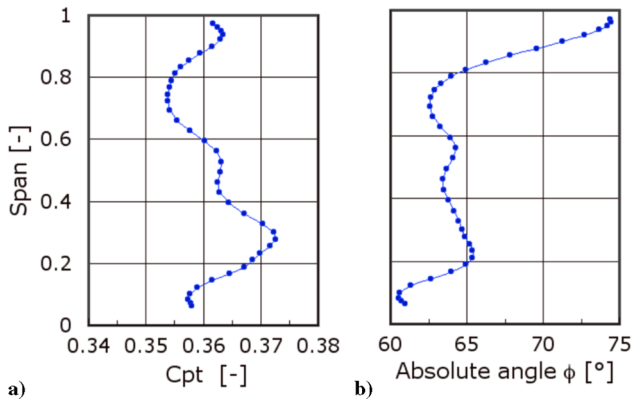

Fig. 5 Mass averaged a) total pressure coefficient and b) yaw angle at the exit of the second stator.

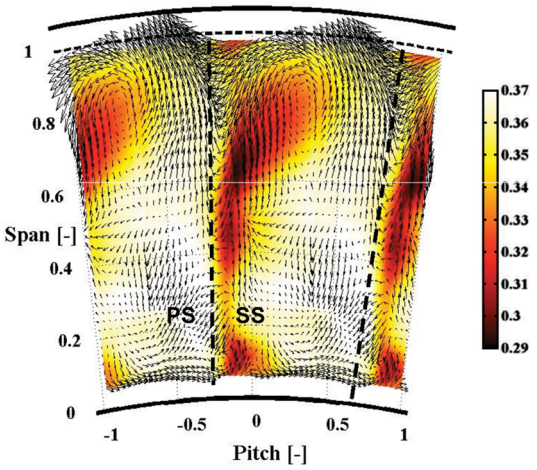

Fig. 6 Measured total pressure coefficient at exit of the second stator.

$$u_{\text{sec}} = u(t) - [\tilde{e} \cdot u(t)]\tilde{e} \tag{16}$$

The velocity u_{sec} is the local secondary flow vector, $u(t)$ the local flow vector while $\tilde{e}$ is the unit vector area averaged and computed at each time step. Each vector is computed in the stationary frame.

The blade trailing edge projection is marked at approximately −20% blade pitch as well as the pressure and suction side. On the pressure side, total pressure coefficient is almost constant along the span and reaches the maximum values of 0.37. Moving circumferentially on the suction side, total pressure reduction is measured corresponding with the secondary flow structures and the wake. The hub passage vortex is identified at the suction side hub and it contributes to the total pressure reduction in this region. Moving further radially, a pronounced loss core can be identified between 0.6 and 0.9 span corresponding with the tip passage vortex. The latter vortical structure is pushing low momentum fluid from the wake radially toward mid height of the blade. In this position, the higher total pressure reduction is measured. Turbulence intensity in this area reaches values around 15% and the Degree of Anisotropy, as shown in the following sections, has the highest value of around 2. At the tip casing, the effect of the stator indigenous passage vortex produced by the new boundary layer can be seen at 95% span in correspondence to the trailing edge wake.

A. Turbulence Analysis

The turbulence level downstream of the second stator was calculated using the isotropic assumption, therefore [Eq. (17)]:

$$\overline{u'^2} \cong \overline{v'^2} \cong \overline{w'^2} \qquad \text{Tu}_{\text{iso}} = \frac{1}{2}\frac{\sqrt{\overline{p_1'^2}}}{\tilde{p}_d} \tag{17}$$

without the use of this assumption, according with the previous derivation, the turbulence intensity can be expressed as [Eq. (18)]:

$$\text{Tu} = \sqrt{\frac{1}{3}\left[\frac{1}{4}\left(\frac{\overline{p_1'}}{\tilde{p}_d}\right)^2 + \left(\frac{\overline{v'}}{\tilde{c}}\right)^2 + \overline{\beta'^2}\right]} \tag{18}$$

To quantify the departures from isotropy, the degree of anisotropy is evaluated by comparing fluctuating components in the three directions. Therefore

$$\text{DA} = \frac{\overline{2u'^2}}{\overline{v'^2} + \overline{w'^2}} \tag{19}$$

Figures 7a and 7b show the turbulence intensity levels calculated with and without the isotropy assumption. In both plots, strong similarities are observed with respect to the total pressure distribution shown in Fig. 6. In the wake and in the secondary flow regions the turbulence intensity is higher with a level up to 16%. Similar levels of turbulence intensity have been measured in axial turbine using hot

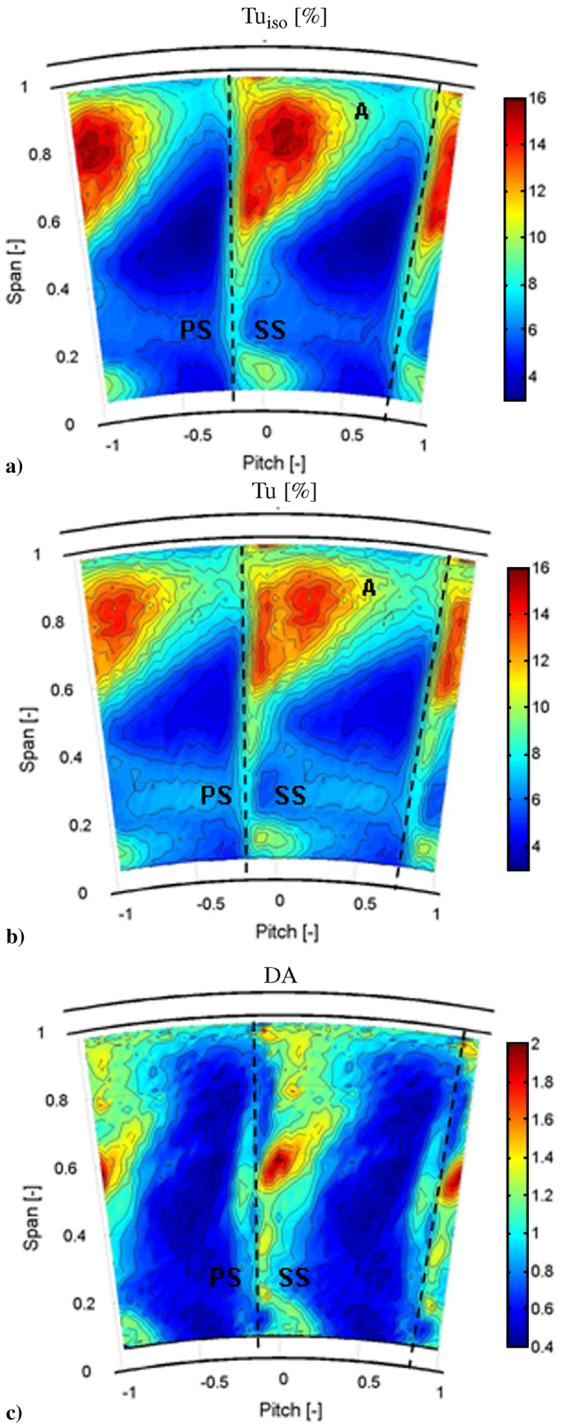

Fig. 7 Turbulence intensities evaluated a) with and b) without the isotropic assumption c) DA.

wire anemometry technology [4,5] and in fundamental studies of turbulent flows with high shear and coherent structures [21].

At midspan, the turbulence intensity evaluated with and without the isotropic assumption shows similar low values (around 4% increasing up to 9% in the wake region). In a large area between 60% span and the tip casing, turbulence intensity reaches maximum values of 16% in a region corresponding with the interaction between the tip passage vortex and the wake as shown in the secondary plot in Fig. 6.

In Fig. 7b at the tip region, the turbulence level without the isotropy assumption has a higher mean value extended for a wider region [A in Figs. 7a and 7b], which is not present in Fig. 7a. This behavior can be explained taking into account that the flow in that region contains a large amount of turbulent fluid coming through the

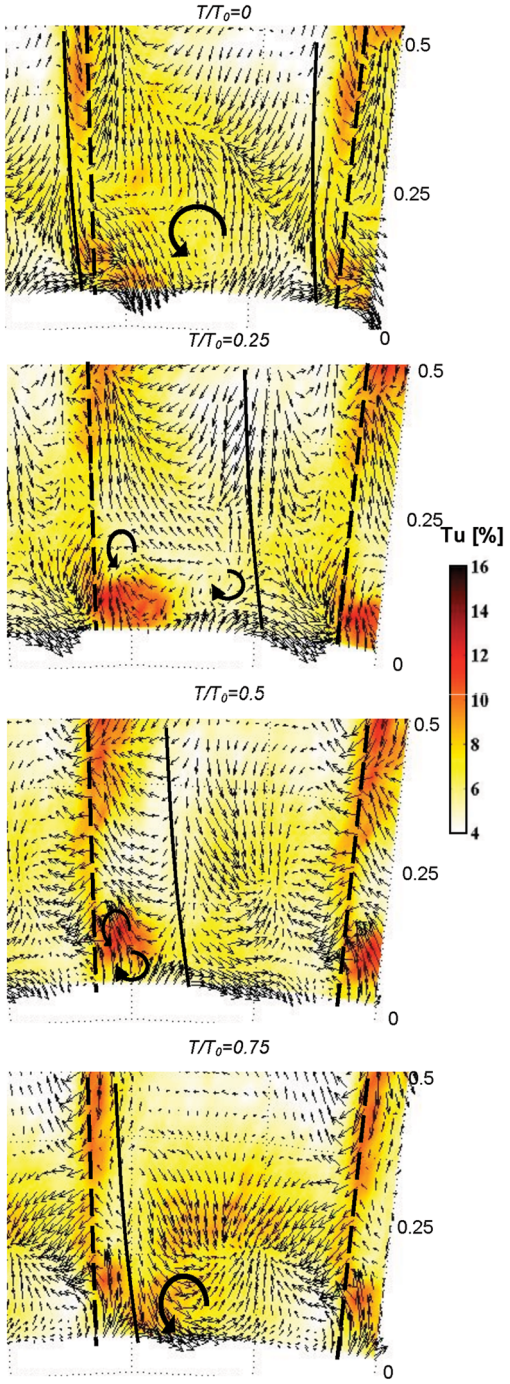

Fig. 8 Measured turbulence intensities and secondary flows in one blade passing period.

first rotor tip. In the same region a high (time-averaged) entropy production has been measured that is not present at the lower part of the blade span.

Figure 7c shows the degree of anisotropy as defined above [Eq. (19)]. Higher values of the degree of anisotropy can be observed at the endwall region and close to the wake. Between midspan and the tip region, toward the blade pressure side where the flow is weakly affected by secondary flows structures, surprisingly the contribution of the term $\overline{w'^2}$ and $\overline{v'^2}$ are higher than $\overline{u'^2}$, the Degree of Anisotropy decreases up to 0.5.

This behavior can be explained by taking into account that in an accelerating and uniform flow as is at midspan of a nozzle guide vane, the streamwise vorticity component is stretched and therefore fluctuations in this direction decrease, although the radial and the circumferential terms are poorly affected by the stretching. Moving circumferentially close to the wake, the streamwise fluctuating term increases rapidly reaching values of degree of anisotropy (DA) larger than 1.2 in the wake and in the hub passage vortex core. In a large region at midspan corresponding with the wake, the DA has the maximum values. This area corresponds with a strong interaction between the tip passage vortex and the blade wake where the DA reaches values of 2 showing that the streamwise fluctuations are locally twice as big with respect to the radial and circumferential terms. At the tip casing, an increase of the DA is as well detected, corresponding with the casing boundary layer.

A high level of anisotropy in secondary flows is also reported by Ristic et al. [7] in measurements inside the turbine rotor. However, in that case, the radial rather than the streamwise term was found to be higher than the other two components both in the wake and in the secondary flow region. This behavior was attributed to the Coriolis forces that tend to increase turbulence intensities in the radial directions inside the rotor boundary layer.

Comparison of the instantaneous turbulence level with the total pressure coefficient shows that regions with high pressure drop as in the wake and in the secondary flows correspond to high turbulence intensity level areas. The maximum instantaneous turbulence intensity reaches the value of 16% of the free stream velocity. Figure 8 shows a close-up of the turbulence intensities in the hub region with the calculated secondary flows superimposed. The position of the projected stator trailing edge is indicated by a dashed line, whereas a continuous line shows the rotor relative leading edge location.

At position $T/T_0 = 0$, a vortex structure at the center of the passage is identified. This vortex appears pronounced in this position and is thought to be the suction side leg of the passage vortex that originates in front of the rotor leading edge. At this position, stator trailing edge and rotor are almost aligned, therefore the area seen by the fluid is the largest. This gives space to the boundary layer to wrap around the rotor leading edge and generate the horseshoe vortex leg rotating in the counterclockwise direction on the blade pressure side. In this position there is a strong interaction with the hub passage vortex of the second stator that rotates in the opposite direction. Because of the interaction of these contrarotating vortex structures, the turbulence level in this area increases up to 16%. It is plausible that the turbulence intensity is increased also due to the acceleration of the passage vortex on the suction side of the rotor blade. During this process, the vortex is first compressed due to the blockage effect of the rotor leading edge and then stretched while accelerating through the suction side of the blade.

This process enhances the production of losses tuned with the blade position due to dissipation effects. Similar unsteady loss generation has already been reported by Chaluvadi et al. [4] where measurement of turbulence is directly related with loss production. The turbulent intensity in the stator wake reaches value up to 12% and is as well modulated by the blade passing period. When the wake is approaching the leading edge of the rotor a compression is occurring due to the blockage effect. If the wake is considered as two vortex sheets, the compression is enhancing the velocity difference inside the wake and therefore mixing losses. A high turbulent kinetic energy is measured during this process at $T/T_0 = 0.5$ while the rotor leading edge is approaching the stator wake.

Absolute values of turbulence intensity derived with the current approach are consistent with LDA or hot wire anemometry measurements performed inside rotor blades (Zaccaria and Lakshminaravana [22] Chaluvadi et al. [4], and Chaluvadi et al. [5]).

At each rotor position, the turbulence intensity levels, the streamwise $\sqrt{\overline{u'^2}}$ and radial $\sqrt{\overline{w'^2}}$ fluctuating components are mass averaged in order to obtain one value at each rotor–stator position. The resulting plots are presented in Fig. 9. All three parameters are plotted at the same scale, same value interval (0.5% of the local mean velocity) but different absolute level.

The mean level of the radial fluctuating component $\sqrt{\overline{w'^2}}$ is higher than the streamwise term $\sqrt{\overline{u'^2}}$ with a difference up to 45%. Significant differences are found in the amplitude of variation of the

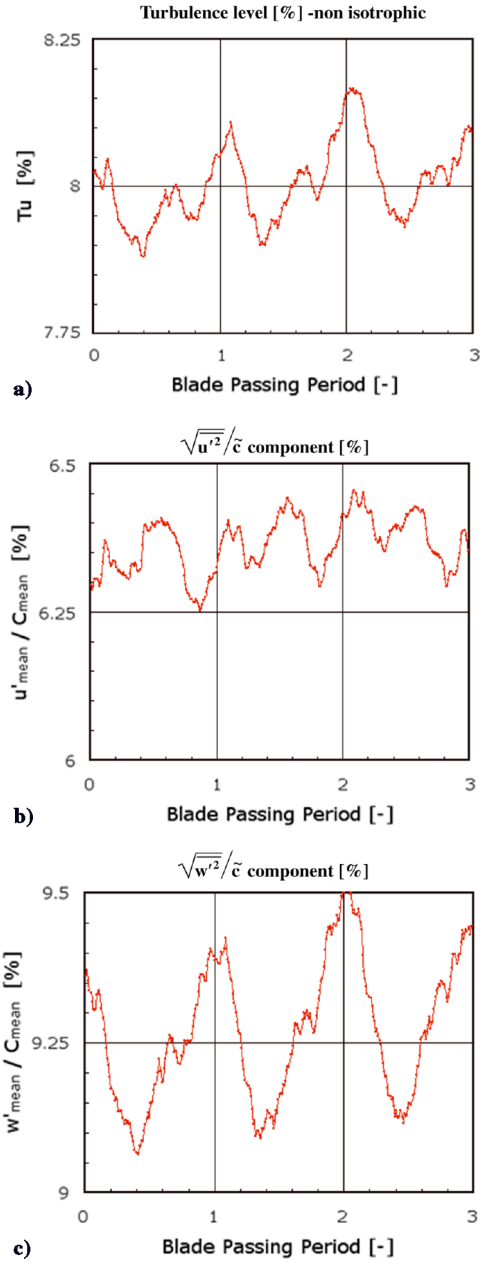

Fig. 9 Measured mass averaged value of a) Tu intensity b) streamwise, and c) radial fluctuating component in 3 blade passing periods.

fluctuating terms. The radial component is varying as function of the blade period between 9% and 9.5%, however, the streamwise variation is limited between 6.25 and 6.45%. Moreover the radial term $\sqrt{\overline{w'^2}}$ shows a clear periodicity as the blade passing period with higher peaks at T/T_0 equal 0 and smaller kinks at T/T_0 equal 0.66. The same peaks are not observed in the streamwise fluctuation. Two peaks of similar amplitude are observed with a frequency twice the blade passing frequency. The interaction between the vortex structures and shed vorticity in the wake contributes to this behavior.

V. Conclusion

In this paper, a novel approach on the measurement of turbulence parameters in turbomachinery is presented. Using the unsteady pressure signal from multisensor FRAP probe the turbulence intensities and Reynolds stress components are measured at the exit of the second stator blade in a 2-stages axial turbine.

The time average turbulence level reaches level up to 14% in the core of the secondary flows and in the wake. These results are consistent with previous measurements on turbines carried out using other measurement techniques. Moreover, a quantification of the degree of anisotropy in turbomachinery flows is made by evaluating turbulence intensity levels with and without isotropy assumption. The level of the mean turbulent kinetic energy in radial $\overline{w'^2}$ and circumferential direction $\overline{v'^2}$ appears in most of the region higher than the streamwise term $\overline{u'^2}$. However, close to high shear stress area the streamwise component is up to twice higher than the other components. By time averaging the kinetic energy terms on the entire flow area, it is shown that the radial component has a higher level up to 45% with respect to the streamwise fluctuation. This underlines that in turbomachinery flows isotropic turbulence models for computations and predictions are not always appropriate.

In the hub region the interaction of the stator passage vortex and the horseshoe vortex of the second rotor raises locally the turbulence intensity level up to 16%. This behavior is occurring periodically with the blade passing frequency.

The current work shows that multisensor FRAP technology can measured turbulence quantities together with unsteady loss generation. The knowledge of these unsteady phenomena in turbomachinery flows is instrumental in further improvements of performances.

References

[1] Radomsky, R. W., and Thole, K. A., "High Free-Steam Turbulence Effects on Endwall Heat Transfer for a Gas Turbine Stator Vane," *Journal of Turbomachinery*, Vol. 122, No. 4, 2000.

[2] Gregory-Smith, D. G., and Cleak, J. G. E., "Secondary Flow Measurements in a Turbine Cascade with High Inlet Turbulence," *Journal of Turbomachinery*, Vol. 110, No. 1, 1992, pp. 1–8.

[3] Volino, R. J., and Hultgren, L. S., "Measurements in Separated and Transitional Boundary Layers Under Low-Pressure Turbine Airfoil Conditions," *Journal of Turbomachinery*, Vol. 123, No. 2, 2001, pp. 189–197.

[4] Chaluvadi, V. S. P., Kalfas, A. I., Hodson, H. P., Ohyama, H., and Watanabe, E., "Blade Row Interaction in a High Pressure Steam Turbine," *Journal of Turbomachinery*, Vol. 125, No. 1, 2003, pp 14–24.

[5] Chaluvadi, V. S. P., Kalfas, A. I., and Hodson, H. P., "Vortex Transport and Blade Interactions in High Pressure Turbines," *Journal of Turbomachinery*, Vol. 126, No. 3, 2004, pp 395–405.

[6] Binder, A., Schroeder, Th., and Hourmouziadis, J., "Turbulence Measurements in a Multistage Low-Pressure Turbine," *Journal of Turbomachinery*, Vol 111, No. 1, 1993, pp. 153–161.

[7] Ristic, D., Lakshminarayana, B., and Chu, S., "Three Dimensional Flow Field Downstream of an Axial Flow Turbine Rotor," *Journal of Propulsion and Power*, Vol. 15 No. 2, 1999, pp. 334–344.

[8] Xiao., X., and Lakshminarayana, B., "Detailed 3D LDV Measurement of Flow Field Near End Wall Inside a Turbine Rotor," AIAA Paper 2001-3975.

[9] Matsunama, T., and Tsutsui, Y., "LDV Measurements of Unsteady Flow in a Turbine Rotor," AIAA Paper 2002-2742, 2002.

[10] Heneka, A., "Entwicklung und Erprobung einer Keilsonde für Instationäre Dreidimensionale Strömungsmessungen in Turbomaschinen," Ph.D. Thesis, University of Stuttgart, Stuttgart, Germany, 1983.

[11] Ruck, G., "Ein Verfahren zur Instationären Geschwindigkeits- und Turbulenzmessung mit einer Pneumatisch Messenden Keilsonde," Ph.D. Thesis, University of Stuttgart, Stuttgart, Germany, 1989.

[12] Wallace, J., and Davies, M., "Turbulence Measurement with a Calibrated Pitot Mounted Pressure Transducer," *Proceedings of the 13th Symposium on Measuring Techniques for Transonic and Supersonic Flow in Cascades and Turbomachinery*, ETH Zurich, Switzerland, 1996.

[13] Gossweiler, C., Herter, D., and Kupferschmied, P., "Fast Response Aerodynamic Probe Measurements in a Turbulent Pipe Flow," *Proceeding of the 11th Symposium on Measuring Techniques for Transonic and Supersonic Flows in Cascades and Turbomachines*, Hochschule der Bundeswehr, Munchen, Germany, 1992.

[14] Laufer, J., "The Structure of Turbulence in Fully Developed Pipe Flow," NACA Rept. 1174, 1954 (updated 1975).

[15] Koeppel, P., "Instatioäere Strömung in Turbomaschinen: Analyse Zeitbhängiger Sondenmessungen," Ph.D. Thesis, Swiss Federal Institute of Technology, Zurich 2000; Rept. 13500.

[16] Porreca, L., Behr, T., Schlienger, J., Kalfas, A. I., Abhari, R. S., Ehrhard, J., and Janke, E., "Fluid Dynamic and Performances of Fully

and Partially Shrouded Axial Turbine," *Journal of Turbomachinery*, Vol 127, No. 4, 2005, pp 668–678.
[17] Schlienger, J., Kalfas, A. I., and Abhari, R. S., "Vortex-Wake-Blade Interaction in a Shrouded Axial Turbine," *Journal of Turbomachinery*, Vol 127, No. 4, 2004, pp 699–707.
[18] Behr, T., Porreca, L., Kalfas, A. I., and Abhari, R. S., "Multistage Aspects and Unsteady Effects of Stator and Rotor Clocking in an Axial Turbine with Low Aspect Ratio Blading," *Journal of Turbomachinery*, Vol 128, No. 1, 2006, pp 11–22.
[19] Porreca, L., Yun, Y. I., Kalfas, A. I., Song, S. J., and Abhari, R. S., "Investigation of 3D Unsteady Flows in a Two Stage Shrouded Axial Turbine Using Stereoscopic PIV and FRAP: Part I: Interstage Interactions," ASME Paper GT-2006-90752, 2006.
[20] Kupferschmied, P., Köppel, O., Gizzi, W. P., and Gyarmathy, G., "Time Resolved Flow Measurements with Fast Aerodynamic Probes in Turbomachinery," *Measurement Science and Technology* Vol 11, No. 7, 2000, pp 1036,1054.
[21] Kalfas, A. I., and Elder, R. L. "Effects of Free Stream Turbulence on Intermittent Boundary Layer Flows," *Proceedings of the 1995 Conference of the International Gas Turbine Institute, ASME Turbo Expo*, 1995.
[22] Zaccaria, M. A., and Lakshminaravana, B., "Unsteady Flow Field due to Nozzle Wake Interaction with the Rotor in an Axial Flow Turbine: Part 1—Rotor Passage Flow Field," *Journal of Turbomachinery*, Vol 119, No. 1, 1997, pp. 201–213.

C. Tan
Associate Editor